Compression Behavior analysis of a 3D printed Honeycomb infill pattern

International Journal of Scientific & Engineering Research Volume 11, Issue 6, June-2020

Abstract

Submitted to Deakin University
Project guide
Ali Zolfagharian

Abhiram Anupindi
abhiramanupindi@gmail.com

Table of Contents

Compression Behavior analysis of a 3D printed Honeycomb infill pattern for ABS and PLA parts

Abstract

The ever-growing Fused Deposition Modelling (FDM) manufacturing is current and the latest trend for its ability to 3D print models without compromising on the dimensional accuracy of the model. This technique has flexibility in altering the print parameters like print orientation, raster angle, print axis, infill density and material layer thickness. Several researches are in progress to develop and improve this technology as it has got great advantage of reducing the material consumption thereby, minimizing high print costs and simultaneously, maintaining the mechanical stability of the model. The primary focus of this project was to study and valuate the compressional behavior of the selected honeycomb lattice pattern by doing a comparative simulation analysis using SOLID WORKS for a basic solid and the infill pattern. The reason for selecting a honeycomb infill pattern was for its greater compression and shear resistance, compact size and isotopic geometry compared to other infill shapes. In this work, the control of print variables, such as infill density, material, layer thickness and print orientation has been evaluated. A series of compressive test specimens with different print characteristics specified in ASTM D695 standards for compression testing of polymer materials were produced using Fortus 400 3D printer. These specimens were tested using Instron Load Frame for compression and recorded the graphical data like compressive stress vs. strain and peak max/min relationship. The results obtained show that print variables influence largely and on the compressional strength of the model, although the behavior is same. By comparing the results from simulation and experimental data, combination of honeycomb infill patterns from PLA material has higher compressive strength compared to ABS material. In this paper, further discussion about the mechanical behavior of each specimen type with specific print configuration is showed and formulated criteria to determine an optimal infill design based on print variables and load conditions.

Keywords

Fused Deposition Modelling (FDM), ASTM D695 compressive standards for plastic, Simulation, print variables, compressive stress vs. strain relationship, optimal infill design

Acknowledgements

The Project SEN720 (Project Implementation and Evaluation) is done under the guidance of Dr. Ali Zolfaghaharian from the Deakin University, Waurn Ponds, Geelong VIC 3216 campus. I am sincerely thankful to Dr. Sara Vahji (Unit Chair) and Dr. Ali Zolfagharian for giving me brief knowledge about the project and continuous encouragement with required guidance and support throughout my project. I also thank Deakin University for its interdisciplinary lab facilities and intelligent staff who have helped me during the induction and giving me a right guidance in completing my experimental analysis of the project throughout 3D printing and experiment testing. My special and humble thanks to my team members Akhil Kumar Pothraj (performed bending analysis on the similar topic) and Akshay Dalal (performed tensile analysis). Although our content and analysis are not same, we shared the same background and helped each other by fine tuning the project and build an effective analysis.

1.0 Introduction

This paper shows the significance and advantages of utilizing a 3-D printing assembling process over customary assembling procedure preparation about its present and potential applications. 3-D printing technology utilizes the procedure of added substance assembling process where items are fabricated layer-by-layer approach, over the cross-area of arrangement of layers (**Berman** 2012). This layer assembling is frequently identifying with Rapid Prototyping technology that is utilized to make parts for long-term consistency. While the workin g of 3D printers is similar to laser or inkjet printers and makes use of feed material in the form of powder or granules building an image or a structure on layer-by-layer basis (Levy, Schindel et al. 2003). The aim of the study is to develop a framework for infill patterns and study relevant background to support the material for fabrication with consistency without compromising on the dimensional accuracy of the model. Infill is an integral part of the object occupied between the shells or walls and usually measured in terms of infill percentage. There are several infill shapes available and among all triangular and honeycomb infill are popular. The infill percentage varies from zero to 100% and 20% is usually the default density for any prototype to work fine. Less is the infill percentage, less capacity to withstand stress and as a result, failure is high. However, infill has too many extrusion issues and does not bind with outer walls effectively resulting in failure. (**Ameta**, **Witherell** et al. 2015).

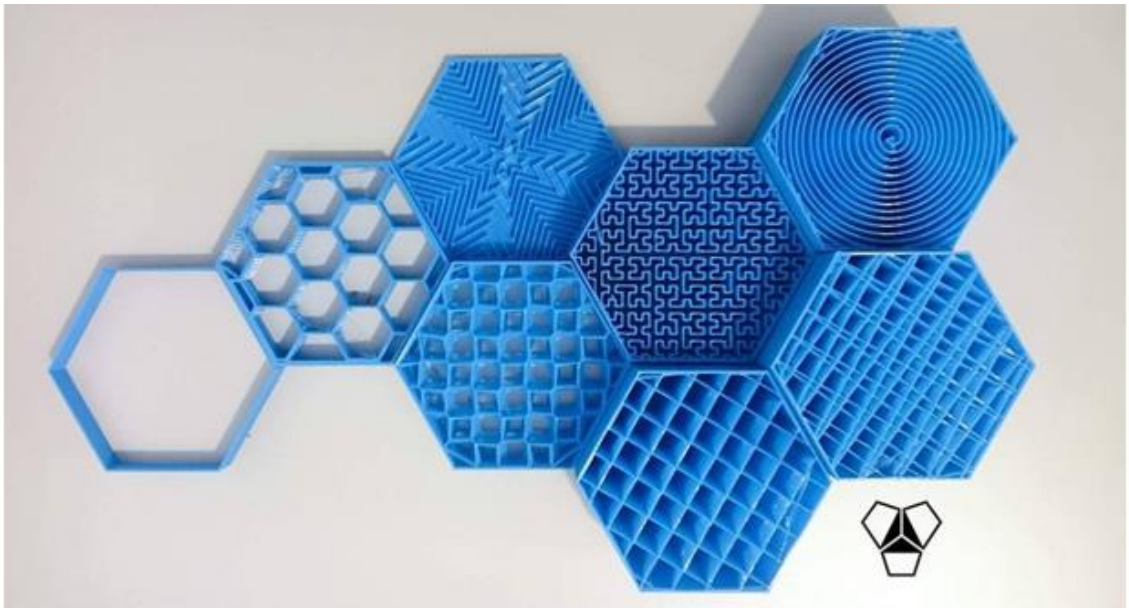

Figure 1: Different infill shapes [Wu, 2019]

The work presented in this paper evaluated different geometric effects of compressive test specimens on the evaluation of isotropic mechanical stability and failure analysis of the model. In addition, relationship between the potential parameters like compressive stress vs. strain and other relevant information associated to different specimen types are presented.

1.1 Project objectives

The primary objective of this project to study the compression analysis of the infill lattice structure and analyze the compressive stiffness results of the compressive test specimens at different loading conditions for different design print parameters. The main project objectives are as follows:

1. Design the hexagonal infill lattice structure using SOLID WORKS modelling software.
2. Perform the compression simulation analysis of basic hexagonal infill lattice using Solid Works software.
3. Observe and record the static distortion results and compare the results for different parameters.
4. Print different infill patterns and test them according to ASTM D695 standards for compression.
5. Perform and record the results for compression testing of different specimens using Instron Load Frame.
6. Formulate criteria to determine an optimal infill design.

1.2 Project deliverables

Task	Completed / Pending
3D modelling a Honeycomb infill lattice using SOLIDWORKS	Completed
Studying the relationship and behavior of influencing parameters	Completed
Simulation of the model using SOLIDWORKS for two different materials ABS PC and PLA	Completed
Data collection of the values such as Von miss stress and strain, displacement, amplitude and vibrational analysis	Completed
3D printing the model for experimental study specified by ASTM D695 Standards	Completed
Level 1, 2 and 3 lab induction and PSA form approval for experimental study (pre-requisites)	Completed
Experimental study for compression using Instron Load Frame for all the specimens	Completed
Comparing results and evaluating the optimum compression modulus for the model and project closure	Completed

Table 1: Checklist of project deliverables

1.3 Why Honeycomb structure?

Generally, Honeycomb structures have greater compression resistance and shear. The structure consists of hexagonal lattice compact and isotropic geometry that facilitates low material consumption. The hexagonal cells are distributed between the adjacent thin vertical walls. Due to its geometry, the overall structure possesses minimal density that provides high compression properties.

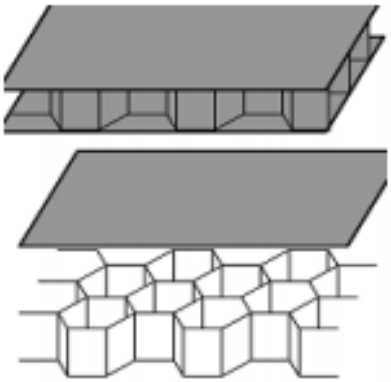

Figure 2: Honeycomb infill structure

Honeycomb structures have wide range of applications like paper-board packaging material, aircrafts, biomedical, snowboards and so on. The key benefits of honeycomb structure are its weight ratio, toughness, fire and high temperature resistant and resistance to moisture. However, manufacturing cost is very high compared to other infill structures because the honeycomb structure has constant and isotropic lattice pattern which takes long manufacturing time.

In the recent years, many researches have been carried out to test the mechanical properties of the honeycomb structure by varying its cell thickness and edges, but the compressive properties of this type have not been well studied. (**B.Vishnu Vardhana Naidu** #1)

2.0Literature review

2.13D printing overview

In simple terms, 3D printing is the process where it prints a three-dimensional solid object in the digital file format. This process is commonly called as additive manufacturing process (AM), where digital file is given as input and the output prints the object layer by layer. Before printing, the model is designed in the form of CAD file that was achieved using SOLID WORKS design software. The model was designed according to ASTM standards for better analysis of the model for all the different types of specimens. There are several types of 3D printing technology depending upon the model requirements and applications. ASTMS have categorized additive manufacturing processes into 7 types and they are as follows:

- Vat Photopolymerization
- Material extrusion
- Powder Bed Fusion
- Binder Jetting

- Sheet lamination
- Fused Deposition Modelling

The overview of all these processes functioning is shown in the below figure. The figure depicts the different stages of operation to obtain the final 3D print. The three stages include sintering, technology and material where these materials are required to start the printing process. Sintering is usually accumulation of the material without the action of melting. (Sachs, Haggerty et al. 1993)

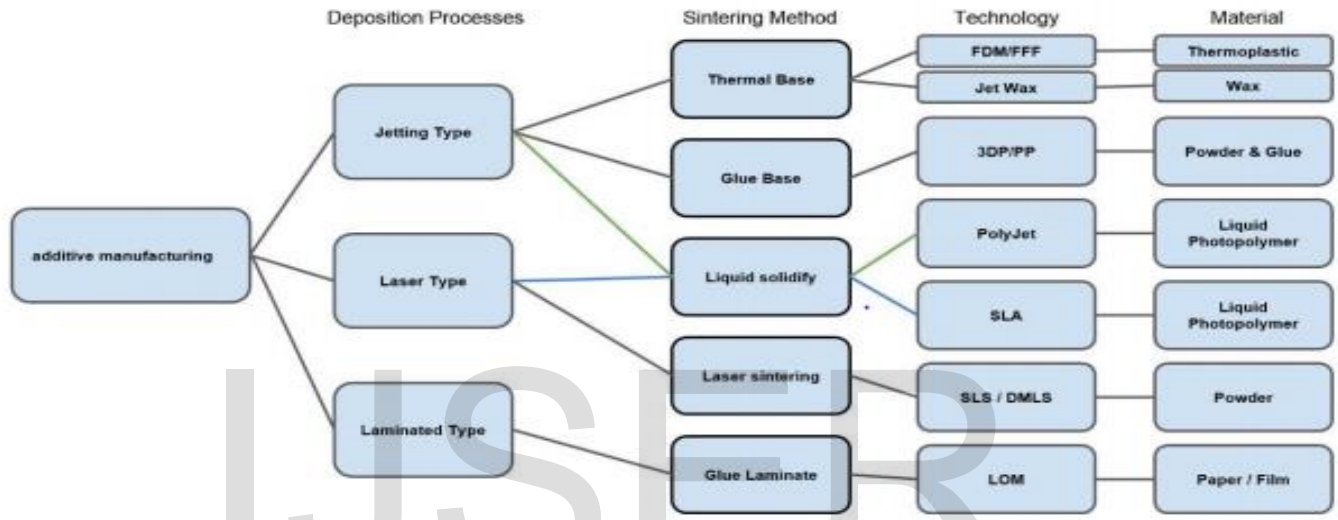

Figure 3: Flowchart of 3D printing technologies. (Sachs, Haggerty et al. 1993)

2.2Fused Deposition Modelling

One of the most commonly used 3D printing technology is Fused Deposition Modelling (FDM) technique where filament is extruded to form the desired 3D model print. This is a part of material extrusion (ME) process. Unlike other 3D printing technologies, this process involves layer by layer material addition to obtain the desired model.

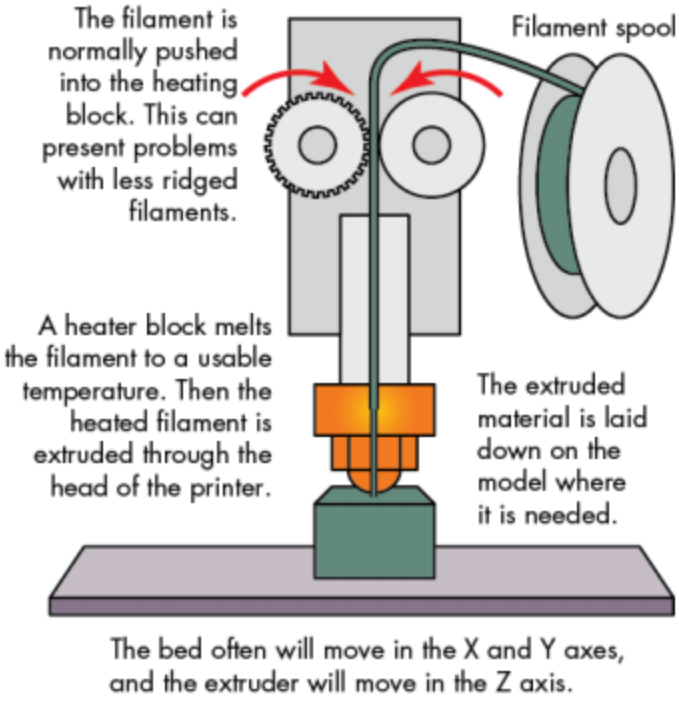

Figure 4: Fused Filament Fabrication process (FFF). (Zein, Hutmacher et al. 2002)

The filament is supplied through the spool and it located near to the printer for easy and fast supply. The filament material used is generally ABS plastic or Polymer that is drawn in the form of wires. The filament is then pushed to the heating blocks with the help of gear arrangement. The heated block melts the filament at a certain temperature and extruded through the nozzle. The nozzle is operated in three different axis X, Y and Z-axis and releases the material layer by layer such that the layer diameter tolerance does not exceed by 1mm. If the filament extruded is very thick then it may congest the nozzle and cause jamming issues. The third dimension begins when the work bed moves a certain distance away from the nozzle i.e. when it reaches the nozzle height. (Zein, Hutmacher et al. 2002)

There are number of applications that needs complex structures and shapes and 3D internal structures to achieve the desired purpose. **Zhang** proposed a fused deposition modelling (FDM) technique to print such complex structure with combinations of polymers, plastics and ceramics. He used "Makerbot® Replicator™ 2X" 3D printer with help of 3D CAD tools to print the complex substrates including waffles, honeycomb and other infill patterns containing air voids. The process involved extruding the thermal layer by heating through the printer nozzle and built the object layer by layer from bottom to top. He filled the patterns with Polylactic acid (PLA) with vertical internal walls at 45^{o} angles with respect to outer walls. The thickness of the both honeycomb and waffle were 0.4mm and cross-sectional thickness

around 0.8mm was chosen. The accuracy of the sample is measured in terms of relative permittivity of the air voids and results showed large PLA volumes showed greater permittivity. (Zhang, Njoku et al. 2015)

Similarly, **Tsouknidas** printed polymeric components using the same fused deposition modelling technique (FDM) to test the density of the infill patterns and relation of energy adsorption with respect to the height of the pattern. He performed the experiment on the cylindrical PLA specimens having 20mm diameter and 30mm height and used the Fused Filament Fabrication (FFF) approach to print the required specimens. Under high velocity conditions of the specimen, the results showed variation in the energy absorption significantly with respect to layer height and apparent density of the specimens. For compression analysis, the energy impact should be sufficiently large to ensure correct results and hence, more than 50% compressive strain is used to determine the impact velocity and mass relationship. The maximum yielding compressive strength is observed to have 0.3mm layer height and 25% infill density and beyond that showed worse compressive response. (Tsouknidas, Pantazopoulos et al. 2016)

Selection of infill design dimensions and thickness is very important as they influence the loading conditions significantly and changes in the mechanical properties of the structure. **Liseli** analyzed the experimental compression, tensile and bending results of several infill patterns with different dimensions and compared the production costs. The study showed that effects of layer thickness, printing orientation and raster angle influence highly on the mechanical properties and greater the layer thickness better is the mechanical properties. The results showed that yield strength and the compressive modulus is higher for the honeycomb structure around 280% compared to other dense structures (Baich, Manogharan et al. 2015). However, the study is confined to only ABS plastic material and further analysis is required to test custom infill patterns for better mechanical testing of different loading conditions. **Osman** conducted experimental study to test the yield strength and compressive modulus of various lattice structures to evaluate the best design using fused deposition modelling (FDM). The specimens were manufactured using Stratasys 3D printer using ABS plastic material having same porosity and thickness for all the specimens. Honeycomb structure showed the best compression properties compared to square, triangle, diamond and circle. The porosity and cell size have huge impact on the yield strength and compression modulus and compared the results for the critical value. The highest yield strength occurred at 0.76 cm edge length and as the edge length increases, porosity increases decreasing the compressive modulus. (Iyibilgin, Yigit et al. 2013).

Other than porosity and thickness of the structure, material properties also play a major role in the modelling analysis. ABS P400 material is found to have a high tensile and compressive strengths compared to polymer and ceramic material. **Sung Hoon** fabricated the parts using FDM 1650 and performed injection molding to formulate experimental results. The compressive strength ranged from 80-

95% for the injection molded parts. The results were compared with FDM based parts and determined the suitable thickness for the parts. The thickness is around 0.013 inch for relatively better compression strength (Ahn, Montero et al. 2002).

Metallic additive manufacturing techniques like Selective Laser Melting (SLM) process can also be used to for fabricating lightweight complex lattice structures. SLM is popular for its ability to build high resolution features of complex freeform geometry using metamaterials. **Chunze** studied the core structure of different cell size ranging from 2 to 8mm to measure the strut density and compression properties. The lattice structures are made of stainless steel and manufactured into required size using CAD software. This made it easy for manufacturing complex lattice structures that are difficult using conventional manufacturing. The inclination angles and the stand thickness are varied for better analysis and gradually increased the space between the layers. The SLM process involves laser melting which induces lot of thermal stress and hence, the structure may lead to deformation or cracking under load application. Therefore, the highest value for the vertical and diagonal struts is found to be 5mm beyond which it may cause to failure or deformation (Yan, Hao et al. 2012). However, SLM is time consuming and has high manufacturing costs for detail and hence, not suitable for commercial applications.

In addition, integrating the biomaterials in the additive manufacturing (AM) technology has evolved and is capable of building complex internal structure with great impact strength. **Thomas** investigated on using a freeform reverse embedded suspended hydrogels called as 'FRESH' that are capable of thermoreversibility, thermoplasticity and high mechanical resistance. These hydrogels are in the form of viscous fluids at higher stress and are built layer by layer heating to 37^{o}C to form the cell friendly object. It works by extruding the FRESH phase material through the syringe into the support bath and later forms into gelatin by cross-linking of the molecules. The 3D printing of FRESH material infill patters is measured in terms of pitch and usually is about 750μm using a repeating geometric structure with specific porosity. The application of these hydrogels are generally used for surgical and medical devices and bone repair (Hinton, Jallerat et al. 2015). However, further research should be done in building complex lattice structures and future engineering using its ability of elasticity thereby having greater compression modulus at different loading conditions.

Although rapid prototyping evolving rapidly, there are certain limitations in the entry-level rapid prototyping machines. **Eujin Pei** examined the problems associated with the 3D printing of complex lattice structures and compared the results to analyze the build parameters. The common problem observed was warping and removal of support material due to complex internal patterns. Also, the precision and surface finish lacked quality. The printed structure are lighter due to its hollow design structure an thus, possess low impact strength than required (Pei, Ian Campbell et al. 2011).

The optimization of fused infill patterns specially for the honeycomb infill structure has not yet been reported. The influencing parameters like material properties, layer thickness, raster angle, infill density and selection of suitable dimensions of the model for better simulation using Finite Element Analysis (FEA) is still needs to be researched.

3.0 General Problem Statement

Based on the literature review, the challenges faced in this project was integrating the load and boundary conditions for the honeycomb isotropic lattice structure and minimize the buckling and warping phenomenon of the structure. Due to buckling, outer walls compress and obstruct complete compression analysis of the model. This project will address the control over the certain parameters like selection of standard dimensions, internal wall orientation and infill density effects that may cause changes in the mechanical properties of the model. The study also helps in achieving maximum and optimum efficiency results without compromising on the quality of the model.

4.0 Methodology

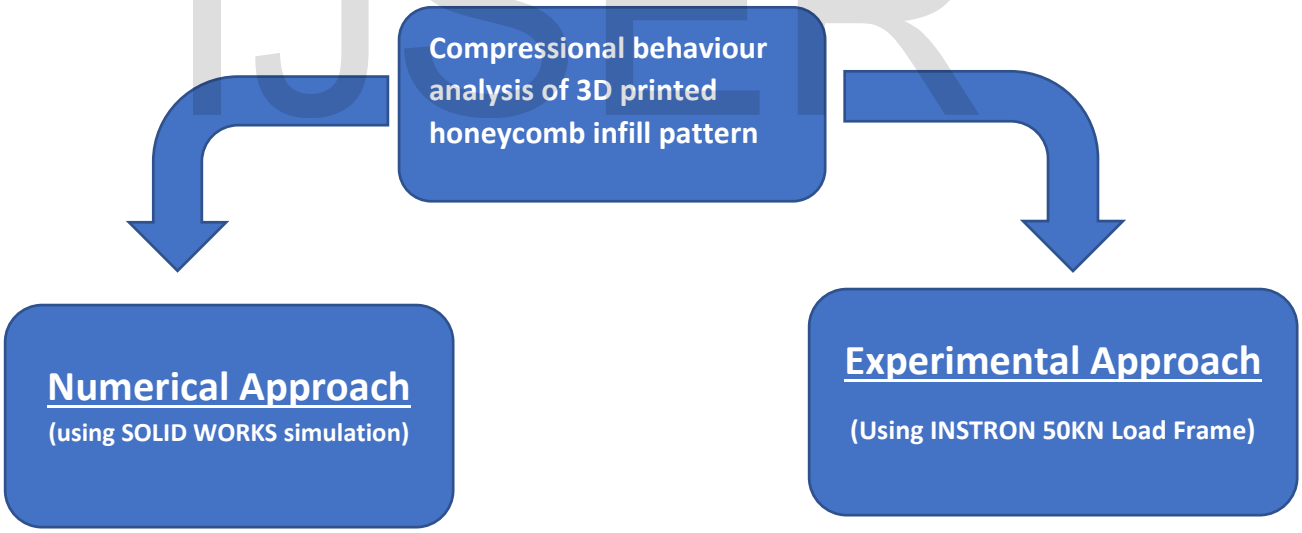

Figure 5: Methodology flowchart

The model was designed based on **ASTM D695 standards** for polymers tested for compression with dimensions having **length = 25.4 mm** and **diameter = 12.7 mm** for a typical cylinder. [ASTM, 2010 #136]

S.NO	Specification	Values
1	Dimensions ASTM	**12.7 x 25.4 mm**
2	Young's modulus of ABS plastic	**2.4 GPa**
3	Young's modulus of PLA	**3.1 GPa**
4	Ultimate compressive strain	**50 MPa**
5	ASTM D695, maximum compressive modulus	**4%**
6	ASTM D695, maximum compressive strain	**3.2%**
7	Equipment used	**Instron Load Frame**

Table 2: Model specifications [ASTM, 2010 #136]

4.1 Numerical approach

4.1.1 Model design

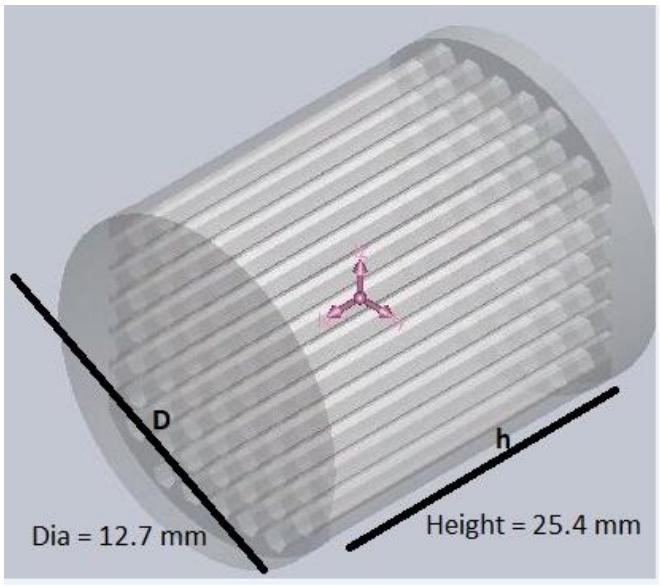

Figure 6: Model design with dimensions

4.1.2 Simulation steps and parameters

The model was designed and extruded such that it facilitated honeycomb infill between the two faces of the model as shown in the above figure 6. The bottom face of the model was taken as selected as a reference edge and grounded and the load was applied downwards i.e. into the model to perform compression perpendicularly to the model at different loading conditions. The density was calculated based on the data given by the modelling software that was around 0.023 g/mm^3 for ABS model having mass around 8.01 grams and density for PLA was around 0.022 g/mm^3 with mass of 7.43 grams. The young's modulus for ABS was taken as 2.3 GPa and for PLA 3.1 GPa with poisons ratio around 0.3 for both the materials. After all the relevant data was given, the model was progressed for static simulation study and analyze the compressional behavior of the model. The steps involved for static simulation are as follows:

1. Create a static study by clicking right-click on study property manager and then click on **create new simulation study**. Click on Adaptive tab to improve the results automatically.

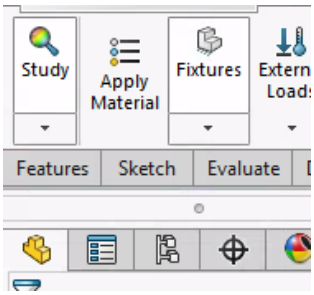

2. Define material for each part i.e. ABS or PLA and right-click on simulation study tree and click on **apply/edit material.**

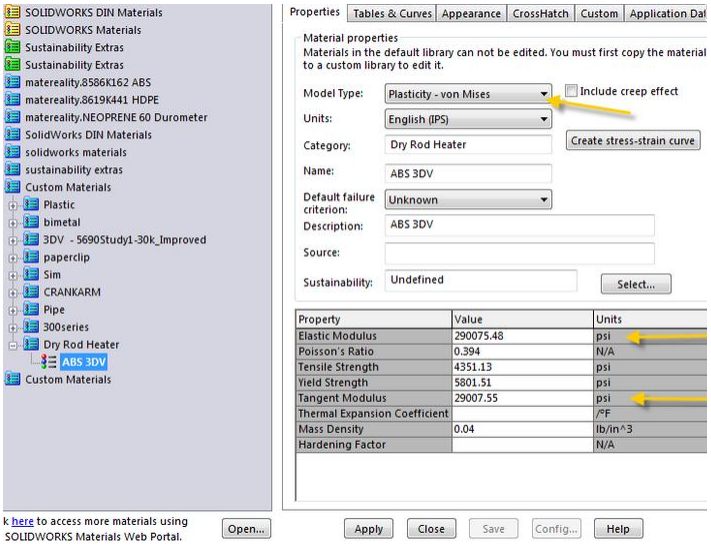

3. Right click on Fixtures icon and define restraints that helps to stabilize contact points and boundary conditions effectively. The bottom face of the model was grounded.

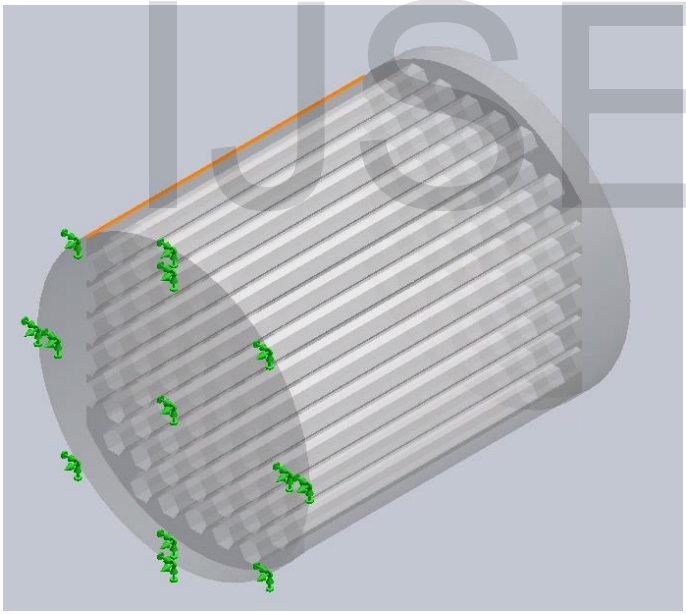

4. Define external loads conditions such as 20N, 50N and 100N for different specimens.

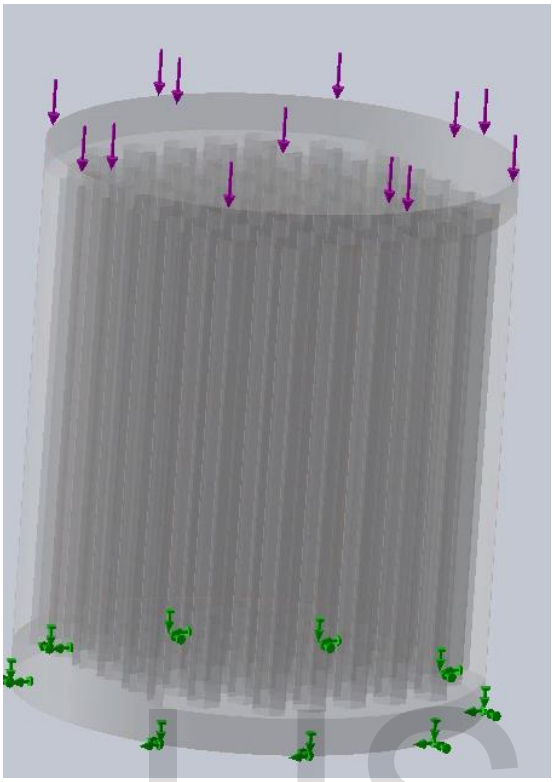

5. Perform mesh i.e. around 3 mm size.

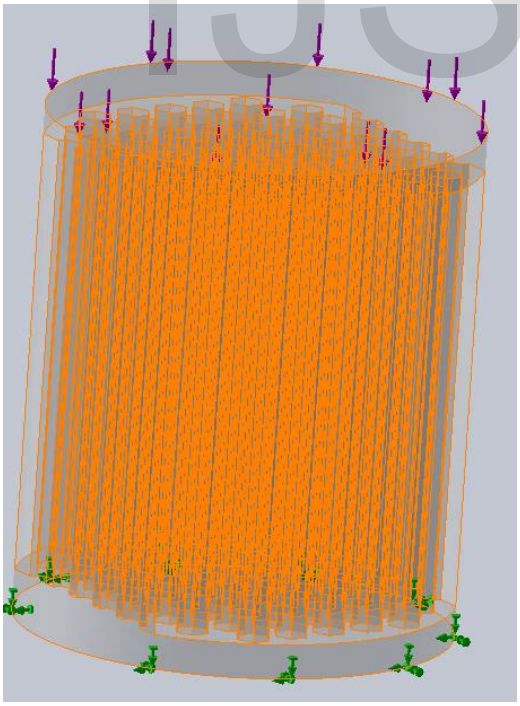

6. Run the simulation study and check for errors.

4.2 Experimental approach

Fortus 400 3D printer for experimental testing produced the compressive test specimens with different print variables such as infill density (25% and 50%), layer thickness (0.1 mm and 0.2 mm), material (ABS and PLA) and print orientation (0^o and 45^o). The .SLD part of the file was converted into .STL file and given as an input to the 3D printed and the printer decodes the file and prints layer-by-layer based on the above relevant information. The 16 specimens with different print configurations were collected after 3D printing was completed.

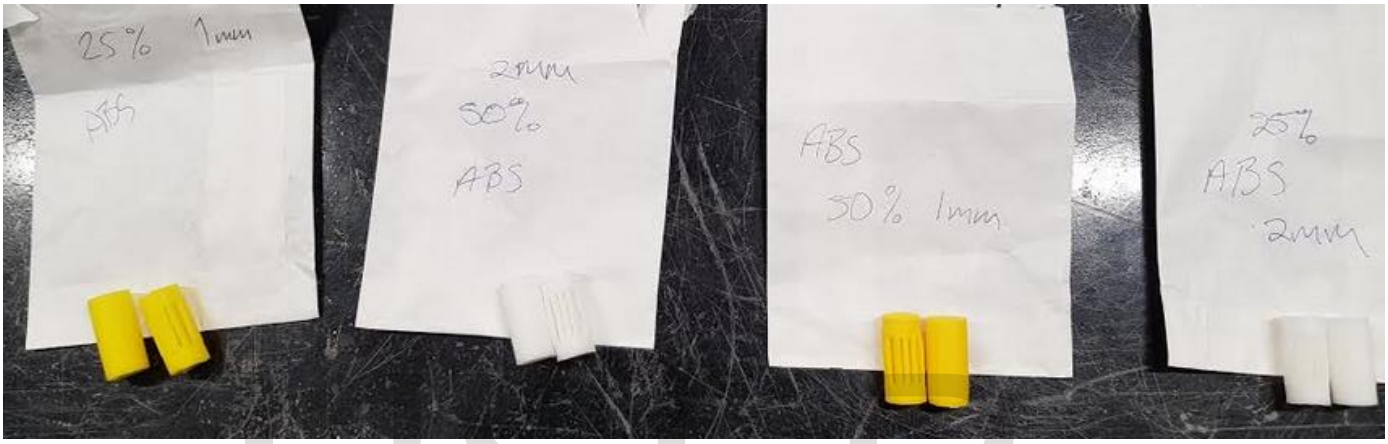

Figure 7: ABS test specimens

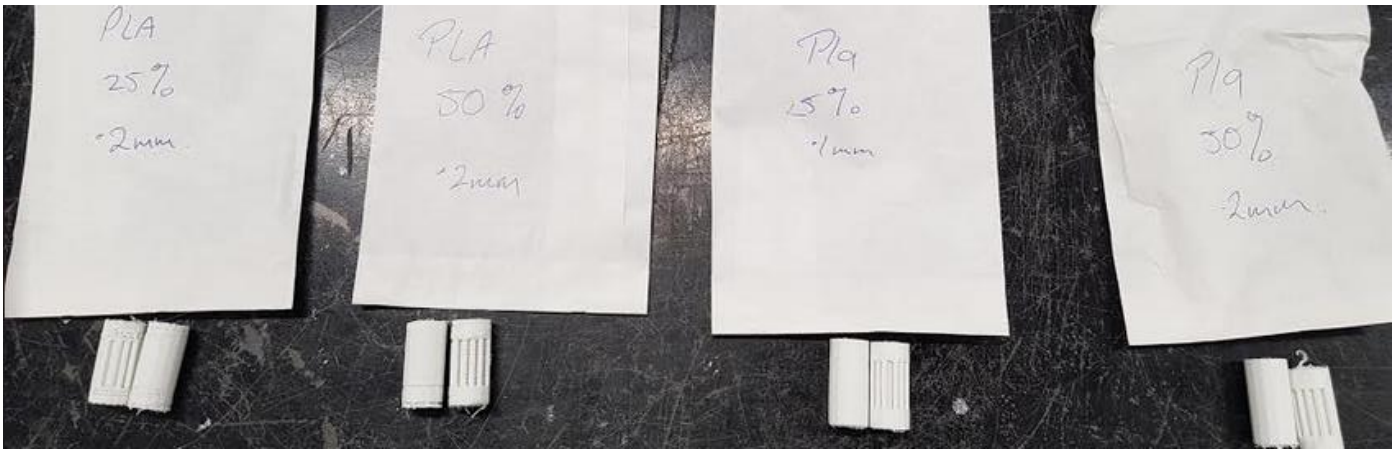

Figure 8: PLA test specimens

4.2.1 Experimental setup and steps

1. First check for suitable fixtures i.e. compression fixture and fix the load cells on the Instron equipment.
2. Turn on the Instron machine and open Bluehill software.
3. Click on balance load and zero the extension.
4. Jog the load cells to a suitable size of the specimen and place the safety notch such that after which the experiment is stopped, and the specimen is protected.
5. Create method and select **compression method.**

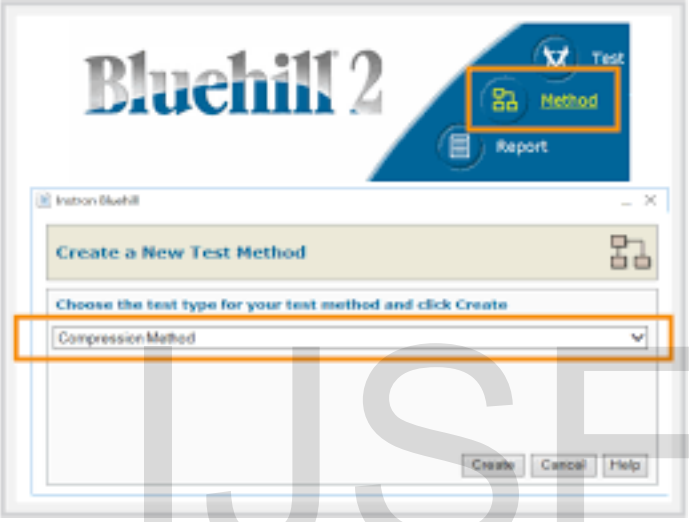

Figure 9: Bluehill compression step manual

6. Fill all the relevant details about sample size, required parameters and graphical results.
7. Run test for the compression method and record the graphical data.
8. Collect the data and compare the results with simulation results to determine the optimal infill design

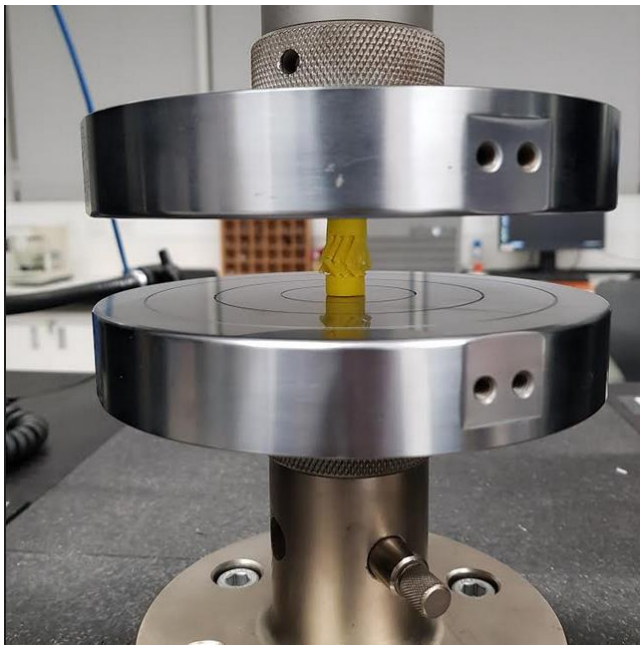

Figure 10: Experimental setup for ABS under compression

Figure 11: Experimental setup for PLA under compression

The experiment is limited up to 2 mm displacement during contraction and beyond that, experiment was stopped. The compression was performed at a ramp rate of 10 mm/min and the compression was stopped when the specimen reached to its 40% failure. All the loads and extension were balanced before the test and the experiment was run for all the specimens sequentially and recorded the relevant graphical values.

5.0 Results

The static simulation analysis for the model specified in ASTM D695 standards for polymers for compression testing was performed and obtained results for extension, Von Miss Stress and Strain, and reaction force. In addition, vibrational analysis was also carried out to define failure point of the model. The model was simulated and studied for different loading conditions 20N, 50N and 100N. The simulation results obtained are as follows:

5.1 Simulation results

5.1.1 Simulation results of 20N load

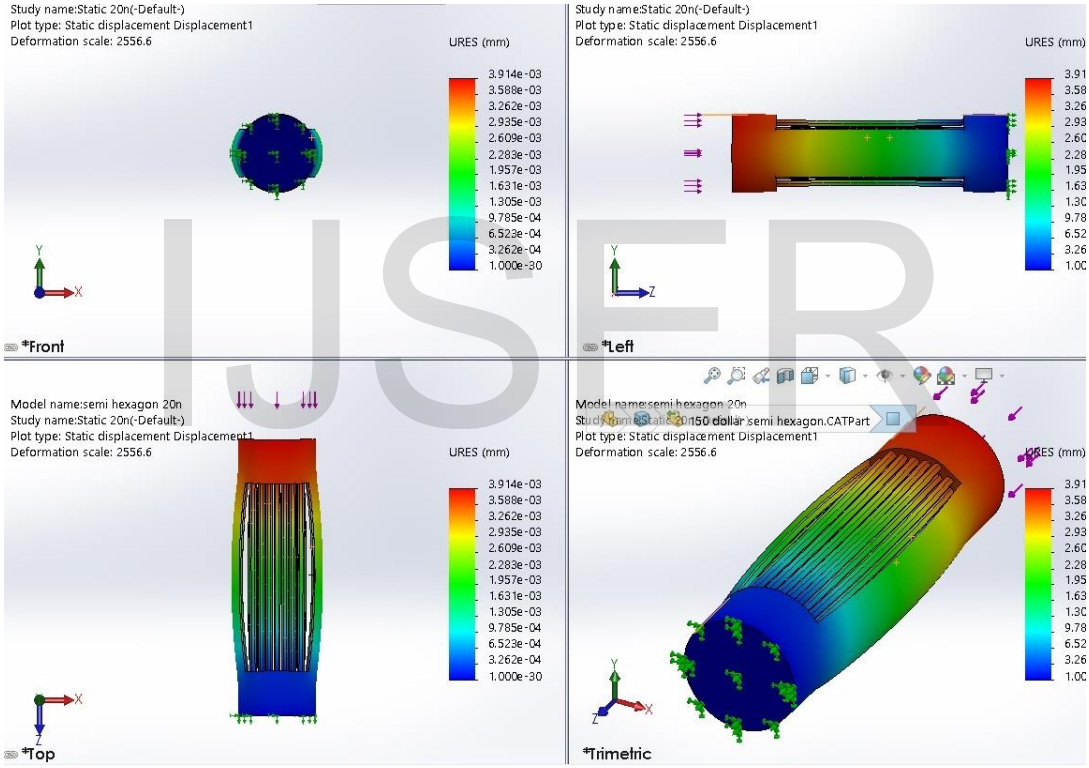

Figure 12: Simulation results for 20N load Multiview

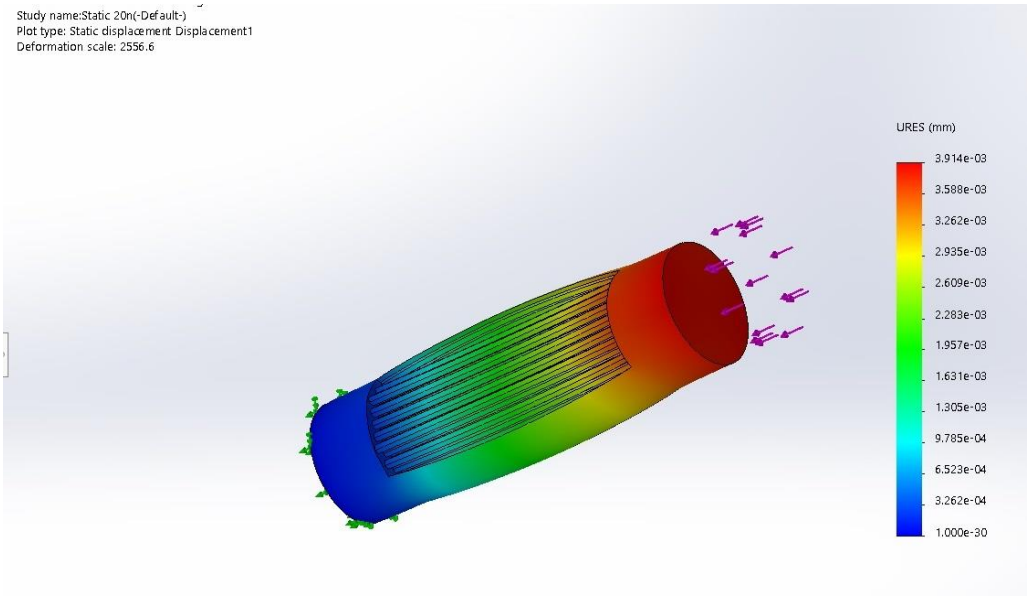

Figure 13: Static displacement for 20N load

5.1.2 Simulation results for 50N load

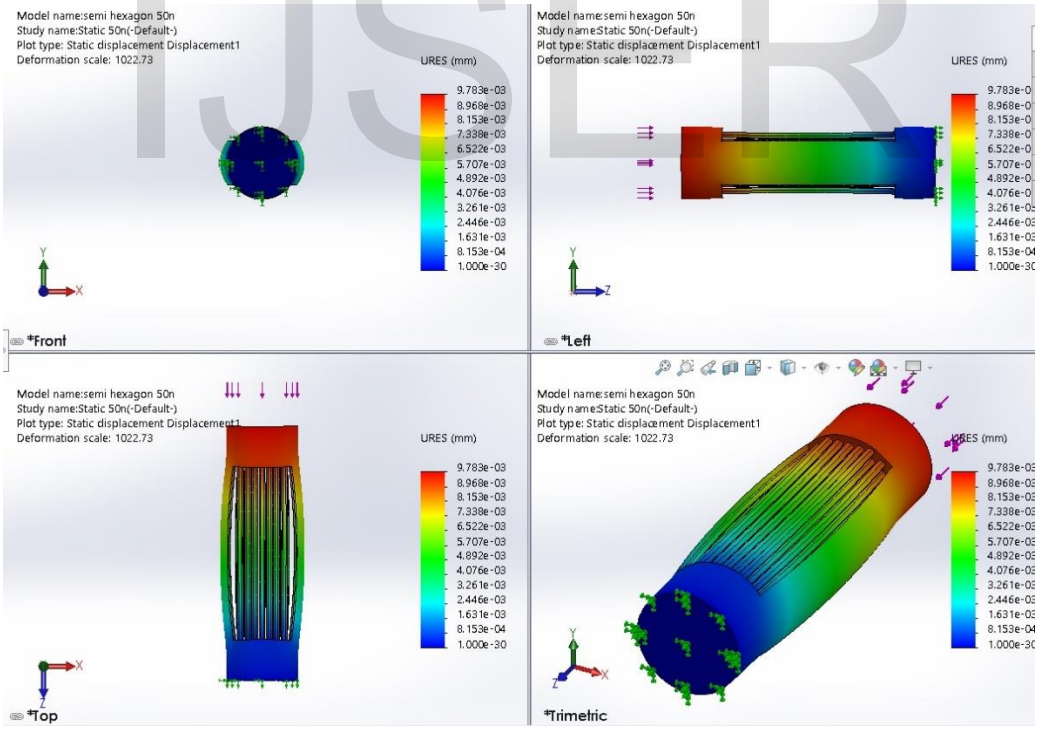

Figure 14: Simulations results for 50N Multiview

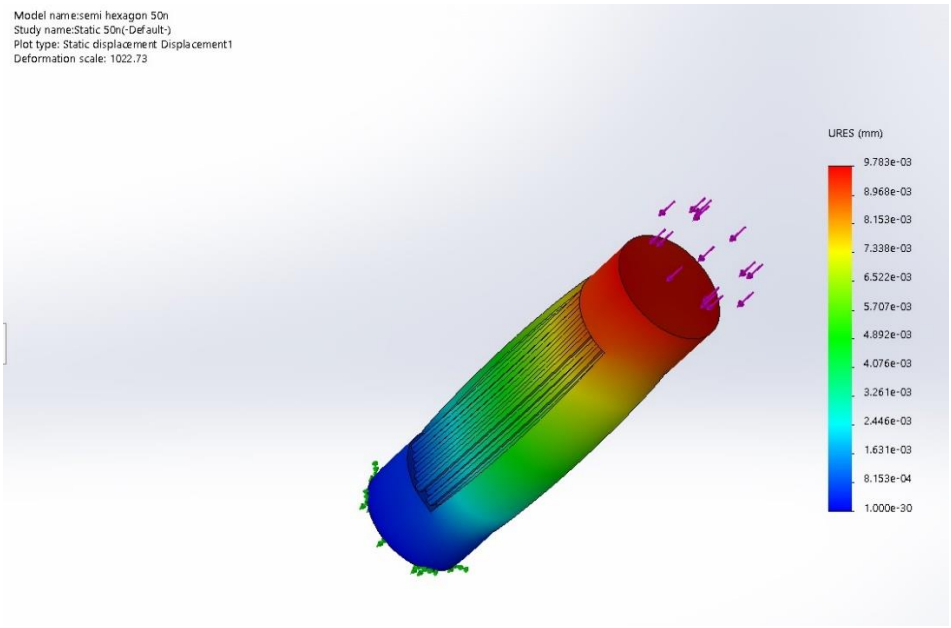

Figure 15: Static displacement of 50N load

5.1.3 Simulation results for 100N load

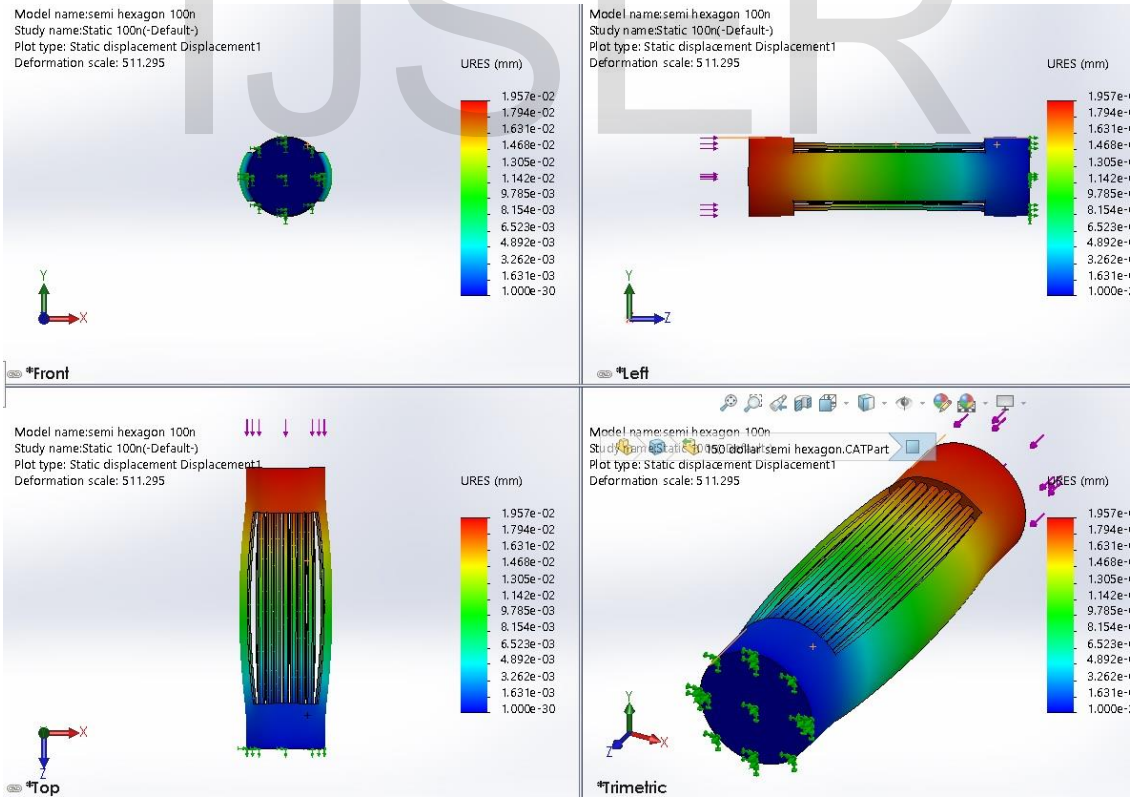

Figure 16: Simulation results of 100N Multiview

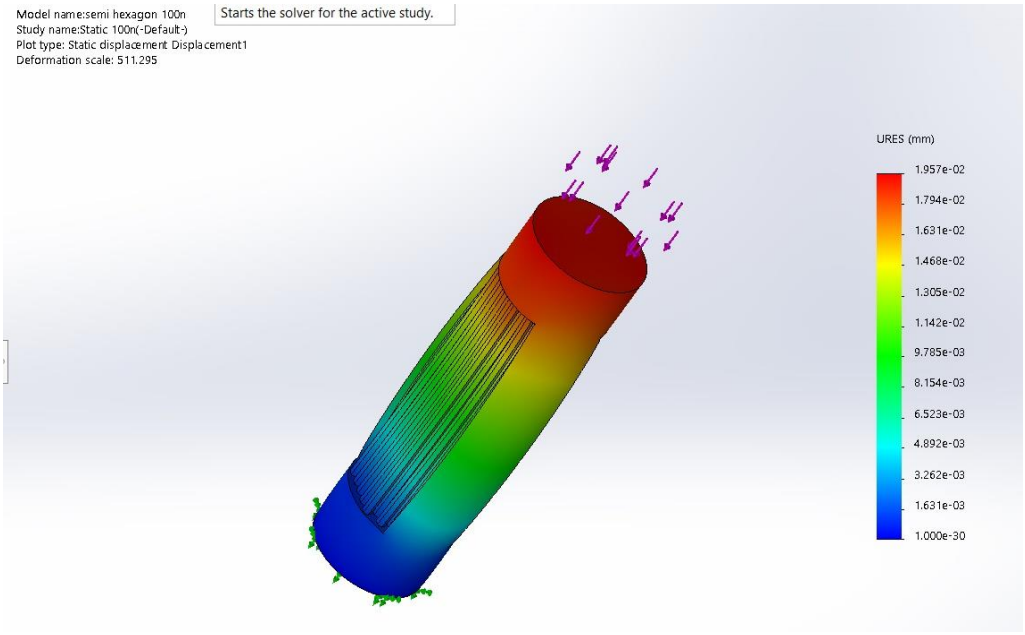

Figure 17: Static displacement of 100N load

5.1.4 Failure point analysis of the model at maximum load (100N)

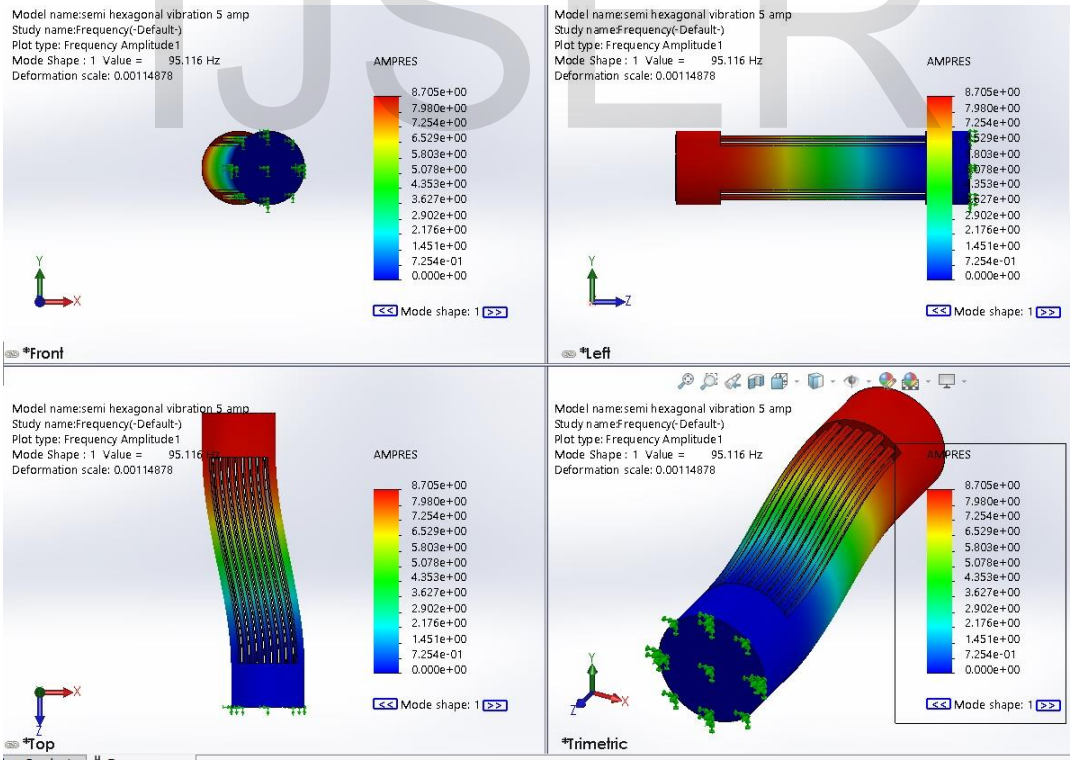

Figure 18: 1st amplitude vibration Multiview

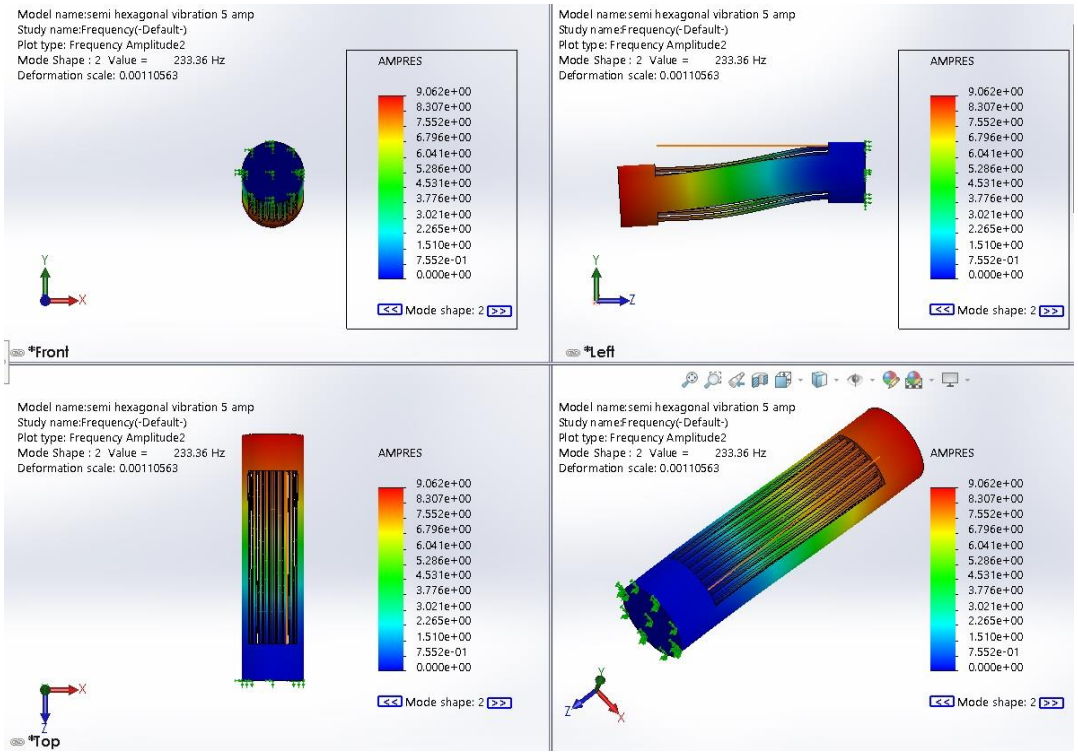

Figure 19: 2nd amplitude vibration

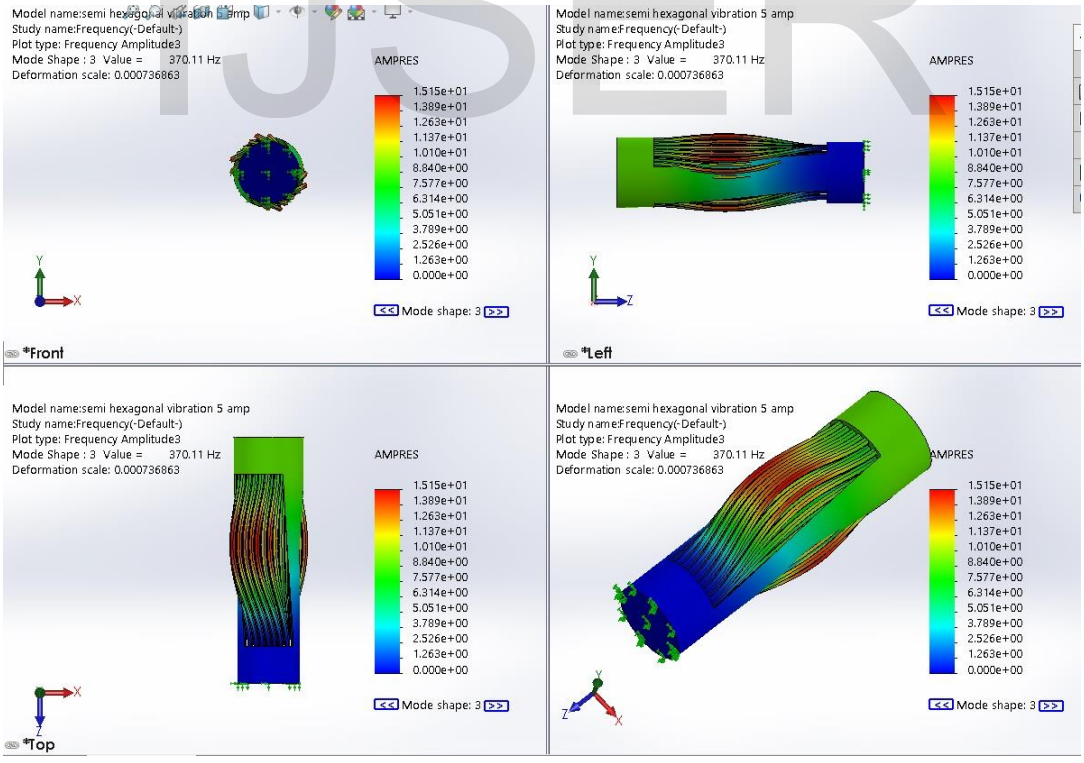

Figure 20: 3rd amplitude vibration Multiview

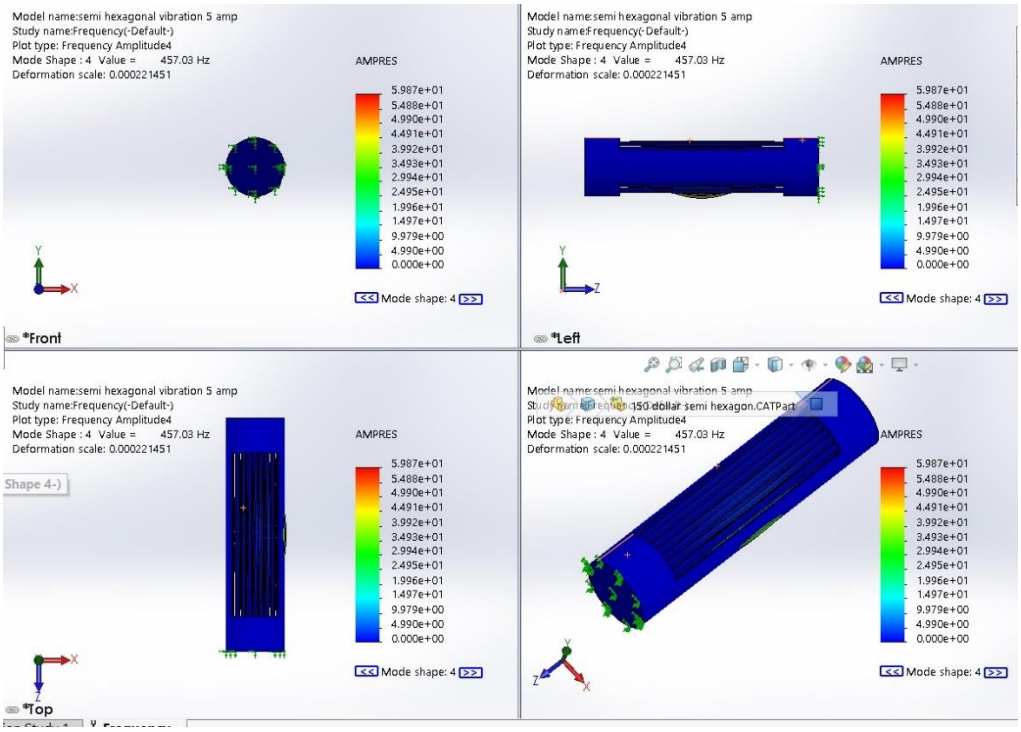

Figure 21: 4th amplitude vibration Multiview

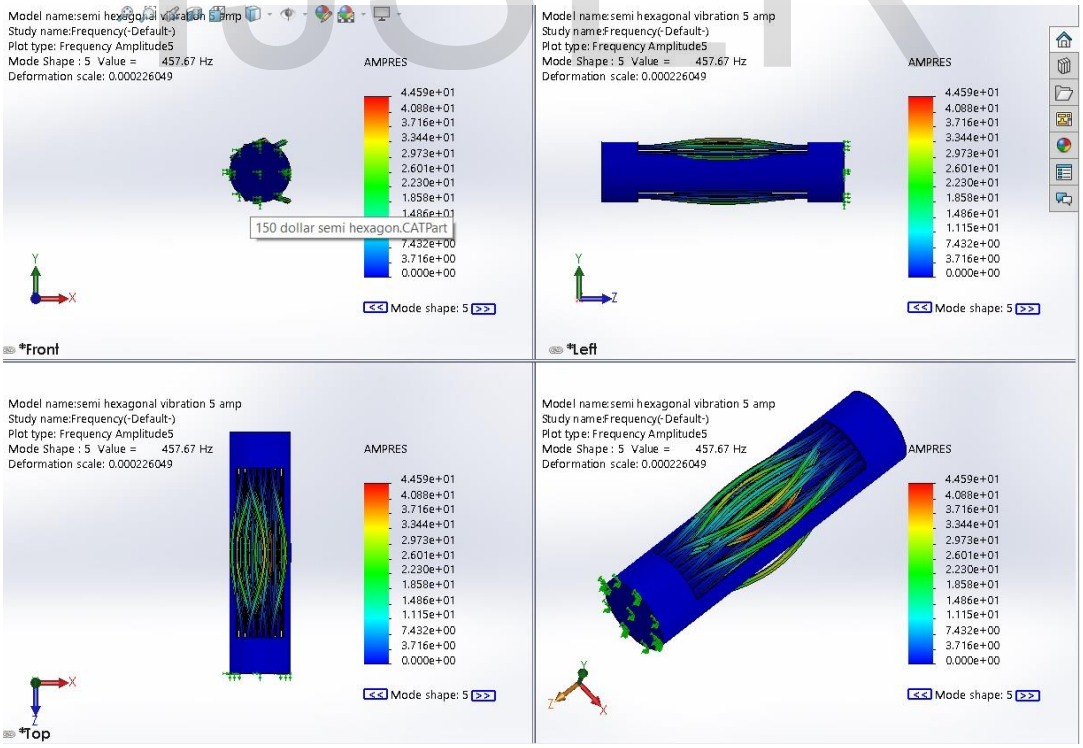

Figure 22: 5th amplitude vibration Multiview

5.1.5 Table of recorded values for simulation

Parameter	Load applied	Maximum Value	Minimum Value
Deformation	20 N	0.3914 mm	0.1305 mm
	50 N	0.9783 mm	0.3261 mm
	100 N	1.957 mm	0.6523 mm
Von Miss stress	20 N	2.456e+005 N/m^2	0.985e+005 N/m^2
	50 N	3.295e+005 N/m^2	1.383e+005 N/m^2
	100 N	6.590e+005 N/m^2	2.767e+005 N/m^2
Von Miss Strain	20 N	0.896e-004	11.546e-006
	50 N	1.184e-004	9.743e-006
	100 N	2.368e-004	1.949e-005

Table 3: Table of simulation values

5.1.6 Simulation compressive stress vs. strain graphical relationship

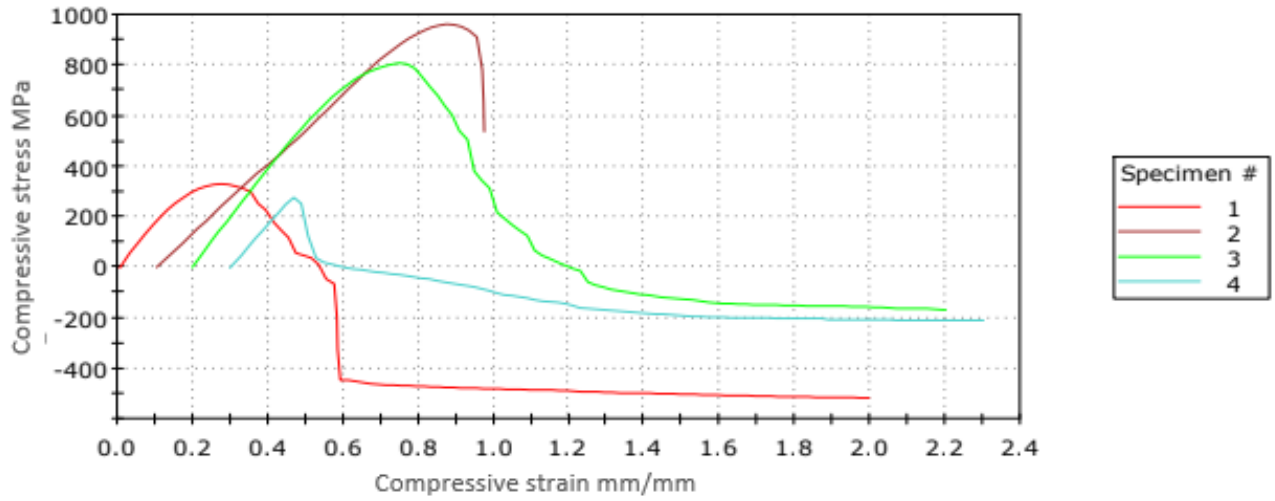

Figure 23: Simulation data graphical representation (Specimen 1 =20 N, Specimen 2 = 50N, Specimen 3 = 100N and Specimen 4 = solid analysis)

5.2 Experimental results

5.2.1 Experimental data for compression of ABS specimens

SNO.	Compressive extension at maximum load [mm]	Compressive strain (extension) at maximum load [mm/mm]	Compressive stress at maximum load [MPa]
1	0.26849`	0.01035	3.12784
2	0.76904	0.02966	9.16478
3	0.55009	0.02121	7.70140
4	0.16933	0.00653	2.62646

Table 4: Experimental results for compression of ABS specimens

5.2.2 Experimental compressive stress vs. strain graphical data for ABS

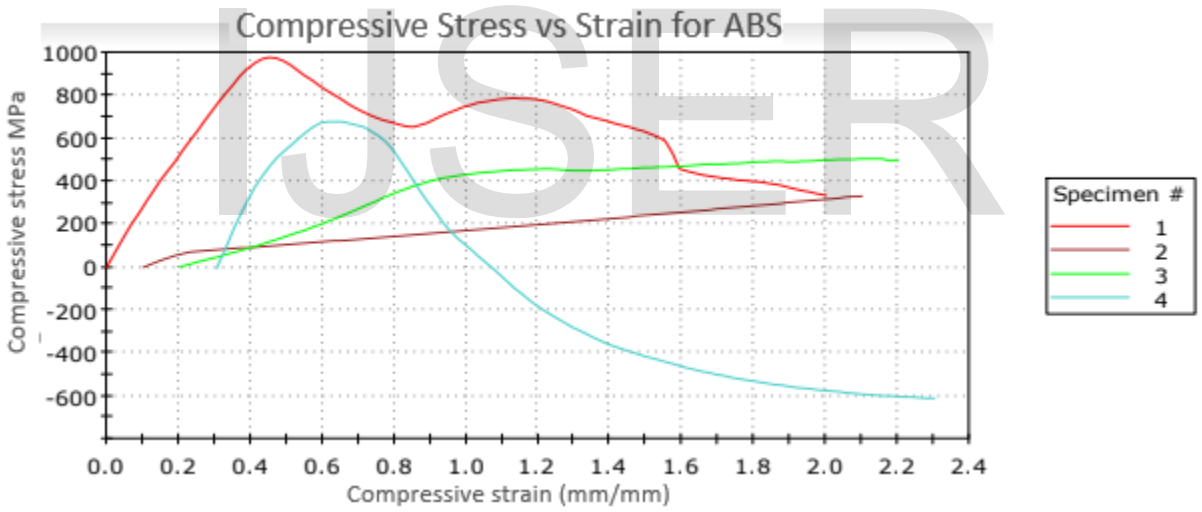

Figure 24: Compressive stress vs. strain for ABS graphical relationship. Specimen 1 = 25% infill with 0.1 mm, Specimen 2 = 25% infill with 0.2 mm, Specimen 3 = 50% infill with 0.1 mm and Specimen 4 = 50% infill with 0.2 mm.

5.2.3 Experimental data for compression of PLA specimens

SNO.	Compressive extension at maximum load [mm]	Compressive strain (extension) at maximum load [mm/mm]	Compressive stress at maximum load [MPa]
1	0.45017	0.01712	7.92083
2	1.99418	0.07584	2.67277
3	1.94833	0.07410	4.10255
4	0.32819	0.01248	5.51108

Table 5: Experimental results for compression of PLA specimens

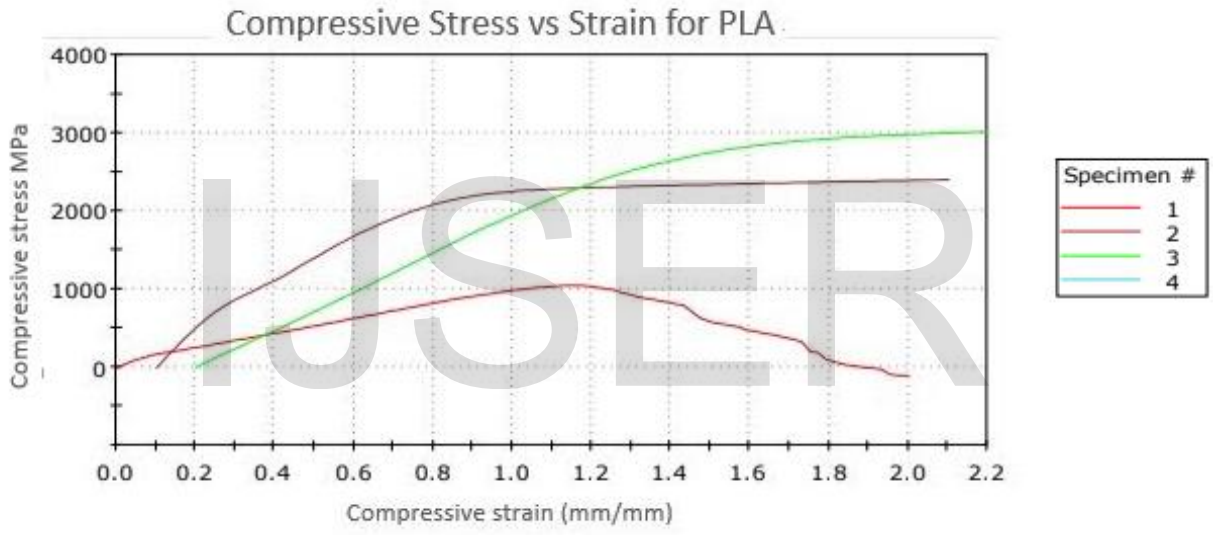

Figure 25: Compressive stress vs. strain for PLA graphical relationship. Specimen 1 = 25% infill with 0.1 mm, Specimen 2 = 25% infill with 0.2 mm, Specimen 3 = 50% infill with 0.1 mm and Specimen 4 = 50% infill with 0.2 mm.

6.0 Discussion

The Compressive stress vs. strain behaviour of specimens of simulation data is shown in Figure 23 with average mechanical properties summarized in Table 3, results show that different loading conditions has influenced material properties of infill designs with different materials. The compressive stiffness is maximum for solid around 2347N and hexagonal infill at 50N of PLA showed greater compressive stiffness around 1458N compared to other specimens. The vibrational analysis was performed to determine the failure point and from the Figure 22, 5th amplitude of the model-analysed failure is mostly occurred at the centre and the model is buckled outwards causing failure at 100N load. These results are

limited to only one print variable type i.e. ABS and PLA and hence, gives limited understanding. Further, the experiment on different specimens with different print variables were tested and showed positive results. Based on the mechanical properties summarized in Table 4 and compressive stress vs. strain relationship shown in Figure 24, the graph exponentially increased which means the specimens are contracting and later graph became negative due to specimen failure. The specimens were observed to fracture at a maximum displacement of 2 mm and beyond which caused failure. Furthermore, based on the mechanical properties summarized in Table 5 and compressive stress vs. strain relationship shown in Figure 25, the graph is accurate and increased in the beginning and became constant that indicates the true property of compression and assumed the specimens employed absolute compression. This nature of PLA specimens deduces true property of compression and prove that they have greater compression resistance compared to ABS specimens. Also, if we clearly observe Figure 24 and Figure 25, compressive stiffness of PLA for specimen 2 (25% infill and 0.2 mm layer thickness) is similar to compressive stiffness of ABS for specimen 3 (50% infill and 0.1 mm layer thickness). This indicates PLA specimen at less infill percentage has greater mechanical strength compared to ABS at 50% infill percentage.

7.0 Conclusion

With growing demand for Additive Manufacturing (AM) technology, it is expected that few more research and innovation in developing printing process and effectively focus on decreasing print costs with high quality output. This project identified the importance of infill pattern specifically honeycomb infill lattice to replace complete solid object and showed positive impact on print cost and material consumption. Multiple influencing print variables like infill density, layer thickness, material and print orientation has been tested and showed that they have the similar mechanical strength and performance compared to solid object. For compression applications, honeycomb infill is more suitable as it as high compression stiffness and weight ratio due to its isotropic geometry. Based on the results and discussions, honeycomb infill of PLA pattern has greater compressive stiffness around 1024N compared to ABS infill pattern which is around 908.1N. This indicates PLA material is more suitable for compression applications and also from the experimental results, findings showed that higher the infill percentage has more mechanical stability is not true in all conditions because PLA specimen with 25% infill percentage and 0.2 mm layer thickness has greater compressional stiffness compared to ABS specimen with 50% infill percentage and 0.1 mm layer thickness. Therefore, compression testing showed a linear-relationship between material properties and the infill percentage. More research should be done to reduce warping and buckling phenomenon. Also, the project analysis is limited only for ABS and PLA material and can be extended for other materials and influencing parameters.

8.0 References

Ahn, S.-H., et al. (2002). "Anisotropic material properties of fused deposition modeling ABS." Rapid prototyping journal **8**(4): 248-257.

Ameta, G., et al. (2015). Tolerance specification and related issues for additively manufactured products. ASME 2015 International Design Engineering Technical Conferences and Computers and Information in Engineering Conference, American Society of Mechanical Engineers.

B.Vishnu Vardhana Naidu #1, G. D. K. "B.Vishnu Vardhana Naidu #1, G. Dileep Kumar #2." International Journal of Scientific Research and Review(2279-543X).

Baich, L., et al. (2015). "Study of infill print design on production cost-time of 3D printed ABS parts." International Journal of Rapid Manufacturing **5**(3-4): 308-319.

Berman, B. (2012). "3-D printing: The new industrial revolution." Business Horizons **55**(2): 155-162.

Hinton, T. J., et al. (2015). "Three-dimensional printing of complex biological structures by freeform reversible embedding of suspended hydrogels." Science advances **1**(9): e1500758.

Iyibilgin, O., et al. (2013). Experimental investigation of different cellular lattice structures manufactured by fused deposition modeling. Proceedings of Solid Freeform Fabrication Symposium, Austin, TX.

Levy, G. N., et al. (2003). "RAPID MANUFACTURING AND RAPID TOOLING WITH LAYER MANUFACTURING (LM) TECHNOLOGIES, STATE OF THE ART AND FUTURE PERSPECTIVES." CIRP annals **52**(2): 589-609.

Pei, E., et al. (2011). "Entry-level RP machines: how well can they cope with geometric complexity?" Assembly Automation **31**(2): 153-160.

Sachs, E. M., et al. (1993). Three-dimensional printing techniques, Google Patents.

Tsouknidas, A., et al. (2016). "Impact absorption capacity of 3D-printed components fabricated by fused deposition modelling." Materials & Design **102**: 41-44.

Yan, C., et al. (2012). "Evaluations of cellular lattice structures manufactured using selective laser melting." International Journal of Machine Tools and Manufacture **62**: 32-38.

Zein, I., et al. (2002). "Fused deposition modeling of novel scaffold architectures for tissue engineering applications." **23**(4): 1169-1185.

Zhang, S., et al. (2015). "Novel 3D printed synthetic dielectric substrates." Microwave and Optical Technology Letters **57**(10): 2344-2346.